JOURNAL OF APPLIED ELECTROCHEMISTRY 20 (1990) 399–404

Studies of the electrodeposition of palladium from baths based on $[Pd(NH_3)_2X_2]$ salts. I. $[Pd(NH_3)_2Cl_2]$ baths

R. LE PENVEN, W. LEVASON, D. PLETCHER

Department of Chemistry, The University, Southampton SO9 5NH, England

Received 22 April 1989

Spectroscopic techniques are used to confirm the chemistry of solutions of $[Pd(NH_3)_2Cl_2]$ in aqueous NH_4Cl at various pH. In addition, potential sweep and step methods at rotating and stationary disc electrodes (both vitreous carbon and freshly plated palladium) are used to investigate palladium deposition from a standard electroplating bath, $[Pd(NH_3)_2Cl_2]$ in NH_4Cl/NH_3 (pH 8.9). The relative importance of oxygen reduction, hydrogen absorption and hydrogen evolution as competing cathode reactions under various conditions is defined and the advantage of strong convection for high rate plating is demonstrated.

1. Introduction

In the last few years, interest in palladium plating has increased substantially, particularly because it is seen as a replacement for gold as a contact metal in the electronics industry. Several alternative electroplating baths for palladium are commercially available and their performance has been compared [1–4]. Perhaps the most common is that based on $[Pd(NH_3)_2Cl_2]$ in aqueous ammonium chloride, pH 7.5–9.0. Despite its widespread adoption, however, little is known about the fundamental electrochemistry of the plating reaction; studies are limited to papers by Hedrich and Raub [5] and Crosby *et al.* [6]. Indeed, there have been very few attempts to use modern electrochemical methods to investigate palladium plating baths although several reports consider palladium deposition in acid chloride media [7–11].

In this paper, we report a study using potential sweep and pulse methods [12] at both stationary and rotating disc electrodes of the deposition of palladium at vitreous carbon and freshly plated palladium. The bath is based on $[Pd(NH_3)_2Cl_2]$ in NH_4Cl at pH 7 to 10. Questions of interest include the effects of varying pH and current density, the influences of oxygen in solution (resulting from air sparging) and of mass transport conditions and the relative importance and effects of palladium hydride formation and/or hydrogen evolution under various conditions. Later papers will compare the behaviour of the chloride bath with those based on $[Pd(NH_3)_2X_2]$ where X is Br or NO_2. The overall aim of this research programme was to improve the selection of the parameters for electroplating palladium.

2. Experimental details

The instrumentation for the electrochemical experiments was a Hi-Tek potentiostat (type DT2101), a Hi-Tek function generator (type PPR1), a Hi-Tek digital integrator, a Nicolet digital oscilloscope (type 2090-111A), a Gould x-y recorder (model 60000) and a EG + G Parc rotating disc system (model 616). Ultraviolet–visible spectra were recorded on Perkin Elmer model 554 spectrometer and pH was monitored with a Kent EIL 7015 pH meter.

The experiments were carried out in two cells. Most used a three-electrode two-compartment cell. The working electrode was a vitreous carbon disc, area 0.07 cm^2, sealed into glass and it was in the same compartment as a Pt wire counter electrode. The SCE reference electrode (Radiometer type K601) was separated from the working electrode by a Luggin capillary whose tip could be manoeuvred close to the surface of the working electrode. The rotating disc experiments were carried out in a cell where each electrode was in a separate compartment. The working and counter electrodes were separated by a glass frit, while the SCE reference electrode was again mounted inside an adjustable Luggin capillary. In this cell the vitreous carbon electrode was a disc, area 0.13 cm^2, surrounded by a PTFE sheath. Before every experiment the vitreous carbon disc electrodes were polished with wet alumina powder (0.05 μm) on a Buehler polishing cloth and then washed with distilled water.

All solutions were prepared with water treated with a Millipore system. The source of palladium was trans-$[Pd(NH_3)_2Cl_2]$ (Johnson Matthey), and BDH Analar NH_4Cl and May and Baker concentrated HCl and 33% NH_3 were also used in electrolyte preparation.

3. Results

3.1. *The homogeneous chemistry of the palladium solutions*

Ultraviolet–visible spectra were recorded for solutions of $[Pd(NH_3)_2Cl_2]$ in aqueous NH_4Cl at various pH

0021-891X/90 $03.00 + .12

Table 1. Ultraviolet–visible spectroscopic data for palladium species relevant to the electroplating bath, at various pH

Solid	λ_{max} (nm)	ε ($cm^{-1}\,dm^3\,mol^{-1}$)
$[Pd(NH_3)_2Cl_2]$	270, 390, 420	–
$[Pd(NH_3)_4Cl_2]$	296, 360	–
Solution		
$[Pd(NH_3)_4Cl_2]$ in concentrated NH_3	297	223
$[PdCl_4]^{2-}$ in HCl	470	–
$[Pd(NH_3)_2Cl_2]$ in NH_4Cl		
pH 2	366(sh), 386	–
pH 4	338, 376	–
pH 7.5	292	196
pH 8.5	292	196
pH 13.6	292	166
pH 8.5*	292	194

* After 3 months.

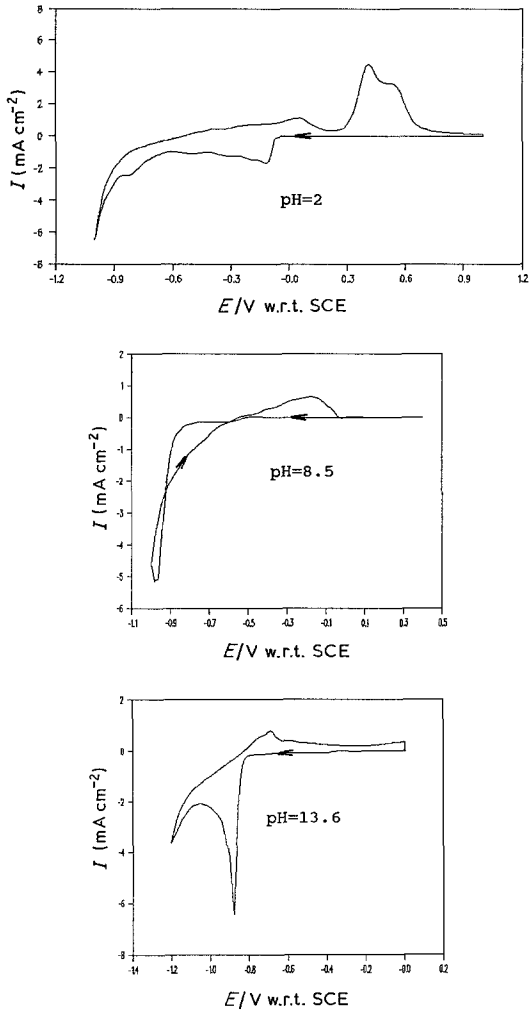

Fig. 1. Cyclic voltammograms recorded at a vitreous carbon disc electrode in 10 mmol dm^{-3} $[Pd(NH_3)_2Cl_2]$ + 1 mol dm^{-3} NH_4Cl at the pH shown. Potential sweep rate 0.1 V s^{-1}.

and also for the complexes $[Pd(NH_3)_2Cl_2]$ and $[Pd(NH_3)_4Cl_2]$ in the solid state. Data from these spectra are recorded in Table 1; the spectra for the two species in the solid state are markedly different, whereas, in general, the wavelengths for the absorption maxima and the extinction coefficients taken from the solution spectra agree well with the data which are available in the literature [13, 14]. It can be seen clearly that in the standard electroplating bath, where ammonia is added to the solution until the pH is 8 to 9, the palladium(II) is present as the tetraamine (which was also the conclusion of Raub and coworkers [2, 3, 5]). The spectrum of the bath is totally unchanged over a period of more than three months suggesting that there is no change in the complexation of the palladium over an extended period. Moreover, the palladium(II) is present as the tetraamine at pH 13.6 and also down to pH 5.0. Below this pH the spectrum of the solution begins to change: initially $[Pd(NH_3)_2Cl_2]$ is formed and in very acid media, $[PdCl_4]^{2-}$ is the major species.

These conclusions are confirmed by cyclic voltammograms of the solution at various pH (see Fig. 1). *I–E* curves for the solutions at pH 13.6, 8.9 and 6.0 are very similar, but below 5.0 the response begins to change. Particularly different is the response at pH 2: there is a large shift in the palladium deposition peak from −0.89 V to −0.11 V. Moreover, in this acid solution, palladium is seen to dissolve anodically and a broad stripping peak is observed. After addition of more acid and the stripping peak becomes sharper and the response resembles closely those reported for acid chloride systems [6–11].

3.2. *The electrodeposition of palladium*

Curve A of Fig. 2 shows a cyclic voltammogram for a solution of 10 mmol dm^{-3} $[Pd(NH_3)_2Cl_2]$ (equivalent to 1 g dm^{-3} Pd metal) in 1 mol dm^{-3} aqueous NH_4Cl at pH 8.9, recorded at 20 mV s^{-1}. Initially, the cathode is a polished vitreous carbon disc and it is rotated at 400 r.p.m. It can be seen that on the forward scan, little reduction is observed until the potential reaches −0.80 V with respect to the SCE when the cathodic current increases rapidly and continuously until the negative limit is reached. The reverse scan is quite different since a well formed reduction wave, $E_{1/2}$ = −0.68 V, can be seen as well as an anodic peak at −0.27 V. The loop in the cathodic current is typical for an electrode reaction involving nucleation and growth of a metal layer on a foreign substrate. Hence, the reduction wave on the reverse scan is thought to be largely due to palladium deposition, although there could be contributions to the cathodic current from oxygen reduction (in line with electroplating practice, the solution was not deoxygenated), formation of palladium hydride (that is, absorption of H_2 in the growing Pd lattice) or hydrogen gas evolution. A major objective of this work was to ascertain the relative importance of the competing reactions under electroplating conditions.

As a first step, voltammograms were recorded for the plating bath without the palladium salt at both vitreous carbon and freshly plated palladium (see curves B and C, respectively, Fig. 2). At vitreous

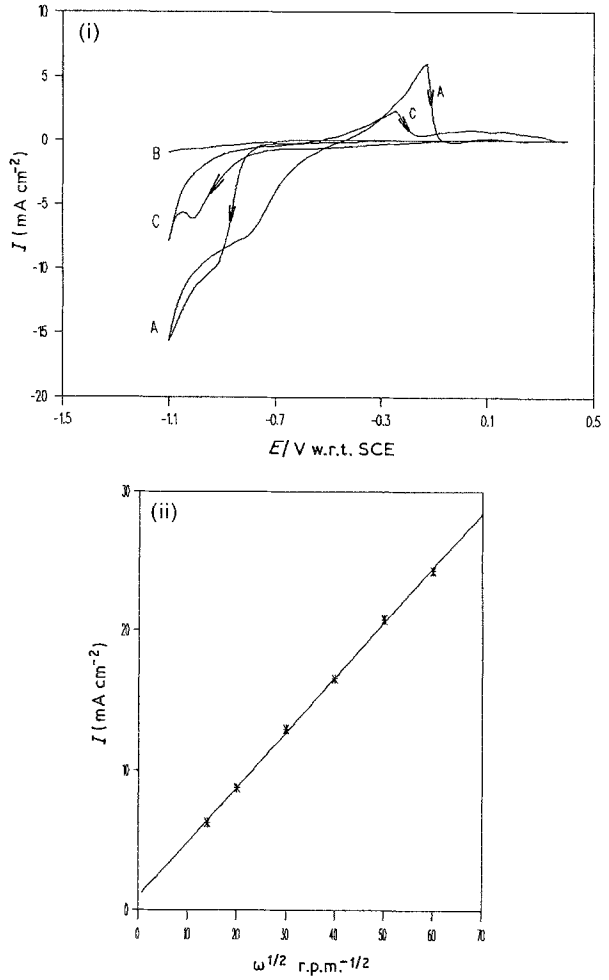

Fig. 2. (i) *I–E* responses recorded at disc electrodes rotating at 400 r.p.m.: Curve A freshly polished vitreous carbon electrode in 10 mmol dm^{-3} $[Pd(NH_3)_2Cl_2]$ + 1 mol dm^{-3} NH_4Cl, pH 8.9; Curve B vitreous carbon electrode; Curve C freshly deposited Pd (100 mC cm^{-2} at −0.80 V in solution used for Curve A) in 1 mol dm^{-3} NH_4Cl, pH 8.9. The dependence of (ii) the current at −0.90 V on the reverse scan as a function of rotation rate for experiment A.

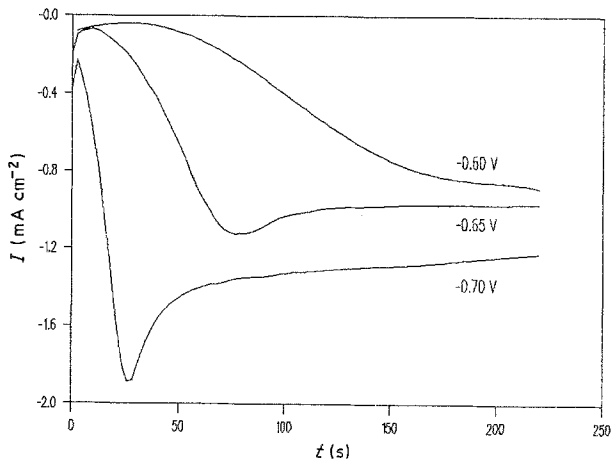

Fig. 3. *I–t* transients in response to potential steps from −0.50 V to the values shown. Stationary, polished vitreous carbon electrode in 10 mmol dm^{-3} $[Pd(NH_3)_2Cl_2]$ + 1 mol dm^{-3} NH_4Cl pH 8.5.

carbon there is no significant background current until hydrogen gas evolution commences beyond −1.0 V. On the other hand, at palladium, two small reduction processes can be seen between −0.2 V and −0.6 V and a larger peak at −0.98 V. It should be stressed, however, that the relative magnitudes of the currents in these experiments do not necessarily represent the relative importance of the processes in the plating situation; for example, it is to be expected that hydrogen will absorb more readily into the expanding lattice during deposition than into the depths of an existing palladium layer.

The experiment of curve A, Fig. 2 was repeated at a series of electrode rotation rates in the range 200 to 3600 r.p.m. The cathodic current on the reverse scan is sensitive to the rotation rate and, indeed, a plot of the current density at −0.90 V against the square root of the rotation rate appears linear (Fig. 2). Moreover, further experiments with palladium(II) concentrations in the range 10 to 40 mmol dm^{-3} show that this current density is also proportional to the palladium(II) concentration. Use of the Levich equation [12], leads to a value for the diffusion coefficient for the palladium (II) species in solution of 10.2×10^{-6} cm^2 s^{-1}. This is, however, a substantial overestimate because no allowance is made for competing electrode reactions which accompany palladium deposition (see below).

The other feature of curve A in Fig. 2 is the anodic peak on the reverse scan. It can be seen that the same peak occurs in the response for the palladium electrode in the palladium free electrolyte (curve C). In principle, this could be a Pd dissolution peak with passivation of the surface, but in fact it was later shown to be the oxidation of the absorbed hydrogen.

The early stages of palladium deposition on a polished vitreous carbon surface were investigated by potential step techniques. The potential was stepped from −0.5 V to a value in the range −0.65 V to −1.00 V and the current–time response was recorded. A typical set of transients are shown in Fig. 3: well formed transients are observed. After an initial rapid fall, the current rises either smoothly to a limiting value, or passes through a peak to a steady state current; as the potential is made more negative, the timescales of the rising part of the transient decrease while the current densities increase. The shape of the initial rising portions of the transients was determined by plotting $(I - I_{\text{minimum}})^n$ against t for various values of n. The best straight lines were obtained for $n = 0.33$, showing that the palladium layer is formed by progressive nucleation and three-dimensional growth under kinetic control [12]. Note that other electrode reactions occurring on the expanding palladium surface increase the current density but do not alter the shape. The linear $(I - I_{\text{minimum}})^{0.33}$ against t plots show an intercept on the t axis which decreases as the potential is made more negative (indicating a delay before the start of nucleation). Figure 4 shows a plot of log slope against E which has a slope of 1/120 mV, consistent with electron transfer as the slow step in the lattice growth.

Figure 5 reports *I–E* curves for a freshly plated palladium electrode in NH_4Cl, pH 8.9, after (a) satu-

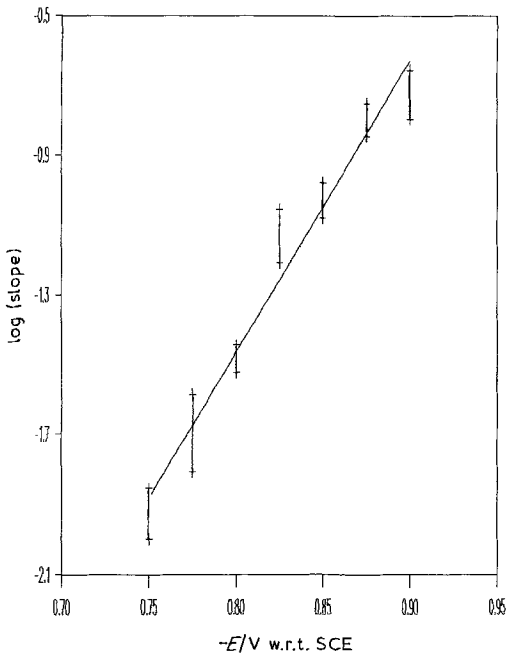

Fig. 4. Potential dependence of the slopes of the linear $(I-I_{minimum})^{0.33}$ against t plots taken from transients such as those shown in Fig. 3.

rating with oxygen and (b) deoxygenating with nitrogen for several minutes. Both curves show the large cathodic peak at -0.95 V and a large hydrogen evolution current negative to -1.0 V. It can, however, be seen that there are two reduction waves for oxygen at -0.11 V and -0.42 V and that the waves are of equal height. Hence the reduction of oxygen occurs by the two step sequence

$$O_2 \xrightarrow{+2e^- + 2H_2O - 2OH^-} H_2O_2 \xrightarrow{+2e^-} 2OH^- \qquad (1)$$

at potentials more positive than those where the reduction of palladium(II) takes place. The height of the oxygen reduction waves increase with the rotation rate of the disc electrode and, at -0.55 V, the current is proportional to the square root of the rotation rate, confirming that oxygen reduction is mass transport controlled at this and at more negative potentials.

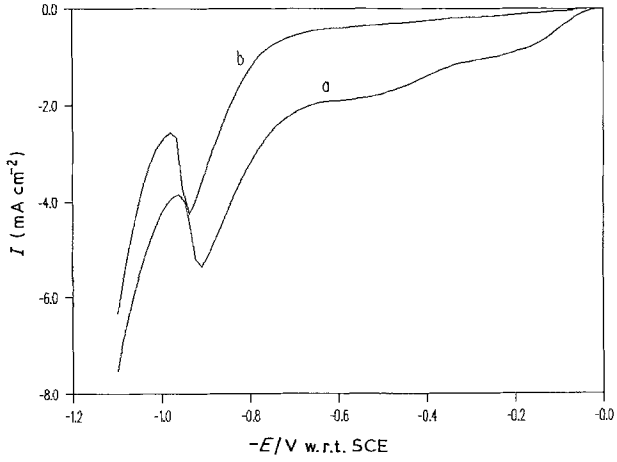

Fig. 5. I–E curves recorded at a freshly deposited Pd electrode in 1 mol dm^{-3} NH_4Cl, pH 8.3: (a) saturated with oxygen and (b) after deoxygenation with a stream of N_2. Rotation rate 200 r.p.m. Palladium deposited by the passage of 100 mC cm^{-2} at -0.80 V in a solution of 10 mmol dm^{-3} $[Pd(NH_3)_2Cl_2]$ + 1 mol dm^{-3} NH_4Cl, pH 8.3.

Again using the Levich equation, we estimate the diffusion coefficient for oxygen as 5.4×10^{-6} cm^2 s^{-1}. Note that, although oxygen reduction takes place at a mass transport controlled rate at potentials where palladium deposition occurs, the solubility of oxygen at room temperature is only 2.2 mmol dm^{-3} and hence the limiting current density for an air saturated electroplating bath is relatively low.

Quantitatively, the relative importance of the other competing reactions (palladium hydride formation and hydrogen gas evolution) during palladium deposition is best assessed by a series of potential step experiments. In the first set of such experiments, the following sequence was followed:

(i) A stationary, polished vitreous carbon disc electrode was placed in a solution of 10 mmol dm^{-3} $[Pd(NH_3)_2Cl_2]$ in 1 mol dm^{-3} NH_4Cl, pH 8.6.

(ii) Its potential was then stepped from -0.5 V to a value in the range -0.74 to -0.90 V and the current and the charge were monitored as a function of time.

(iii) After the passage of 100 mC cm^{-2}, equivalent to the deposition of a palladium layer some 0.1–0.2 μm thick, the potential was stepped back to -0.5 V in order to estimate the amount of $Pd(H_2)$ formed [3, 5].

(iv) The freshly deposited palladium electrode was then washed with distilled water and transferred to NH_4Cl, pH 8.9, without the palladium(II) and the

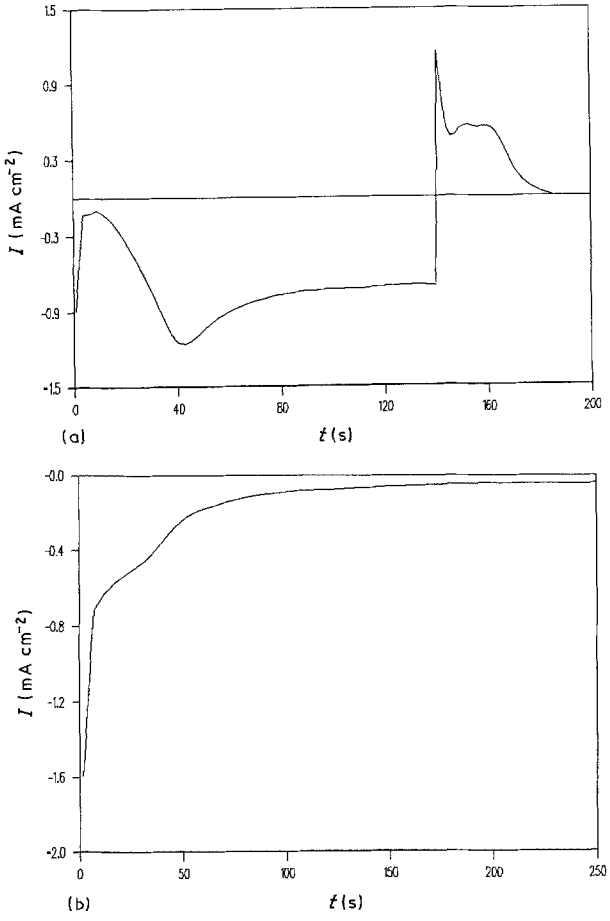

Fig. 6. I–t response to: (a) a potential step sequence from -0.50 to -0.74 V and then to -0.50 V (after the passage of 100 mC cm^{-2}) at a vitreous carbon electrode in a solution of 10 mol dm^{-3} $[Pd(NH_3)_2Cl_2]$ + NH_4Cl, pH 8.6; (b) a potential step from -0.50 V to -0.74 V, following the transfer of the electrode to 1 mol dm^{-3} NH_4Cl pH 8.9.

step from -0.5 V to the potential of interest was repeated. Again the current was monitored as a function of time.

Figure 6 shows the current–time response throughout these experiments for a deposition potential of -0.74 V. The following features should be noted. (a) Following the initial step, the expected rising I–t transient is observed as nucleation and the early stages of growth occur. The current then passes through a peak after about 40 s and falls to a steady state value. The passage of 100 mC cm^{-2} takes about 140 s. (b) On changing the potential to -0.50 V, the current crosses the zero current line and oxidation is observed. The response, where an almost constant current is observed for 20 s and then drops to zero, is that expected for the removal of the hydrogen from the palladium lattice. Indeed it is the shape of this transient which confirms that the anodic peaks in the voltammograms of Figs 1 and 2 are due to removal of hydrogen from the lattice. The charge required for removal of all the hydrogen is 16 mC cm^{-2} at this potential. (c) In the final experiment in the Pd free electrolyte, two electrode reactions, reabsorption of hydrogen into the lattice and hydrogen gas evolution, predominate. The former will only occur until the lattice is fully saturated with hydrogen and this explains the shape of transient recorded. The current thereafter gives the rate of hydrogen gas evolution; the value was read after the same period of time as used for palladium deposition and in later calculations it was assumed that hydrogen evolution occurred at this rate throughout the deposition process.

Figure 7 shows two plots of the current for hydrogen gas evolution and the charge for hydrogen absorption as a function of potential. The plots are continued to slightly lower deposition potentials by including a short pulse (2 s) at -0.90 V prior to the deposition to ensure the rapid nucleation of palladium centres. It can be seen that neither hydrogen evolution or palladium hydride formation are significant reactions positive to -0.67 V. Negative to this potential, palladium hydride begins to form while hydrogen gas evolution increases in importance negative to -0.75 V. At -0.80 V, the data leads to a current efficiency of 54% for palladium deposition and the ratio of H_2 : Pd in the metal lattice may be estimated as 2 : 5. Along the plateau of the Q–E plot, the hydrogen content of the palladium hydride appears to increase from 40 to 60%. These values are close to the maximum found for β-Pd(H_2).

Hence, positive to -0.67 V, oxygen reduction is the only competing reaction. In this region the rate of palladium deposition was investigated as a function of potential. Over the range -0.58 V to -0.68 V, a palladium layer was grown at each potential (although nucleation was initiated by a 2 s prepulse to -0.90 V) and the steady state current was read when the palladium deposition charge was 100 mC cm^{-2}. In the range -0.50 V to -0.57 V the technique was modified slightly; the palladium layer was then grown to 100 mC cm^{-2} at -0.65 V and the potential was then stepped back to the value of interest. The steady state current was read after 40 s at this potential. Figure 8 shows this current–potential data. In addition, it shows the data at more negative potentials (the charge for Pd(H_2) formation has been converted to a current

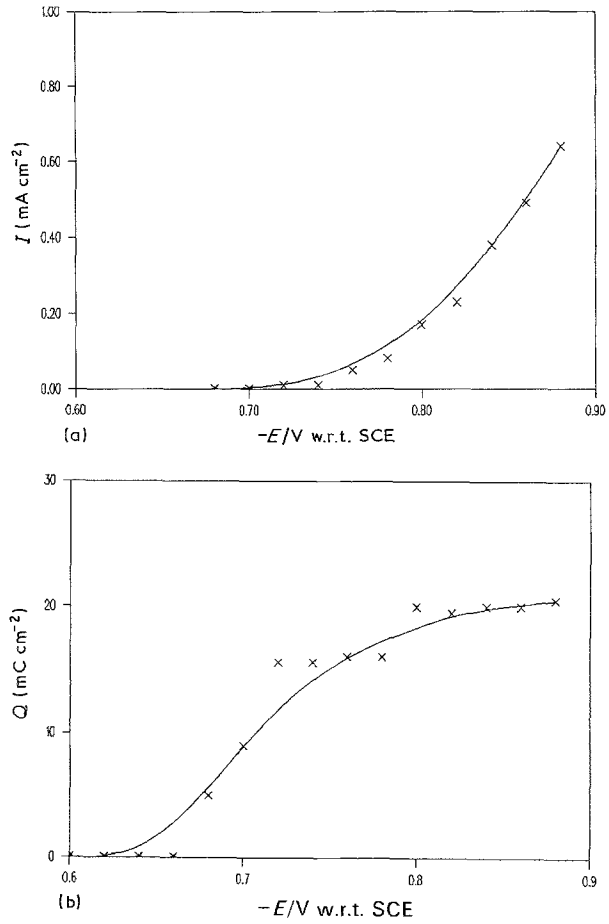

Fig. 7. Plots of (a) current density for steady state hydrogen evolution estimated from the transient of Fig. 8b as a function of potential and (b) charge for H_2 absorption into the Pd lattice during the deposition of Pd as a function of potential (total charge, 100 mC cm^{-2}). Solution composition as in Fig. 8.

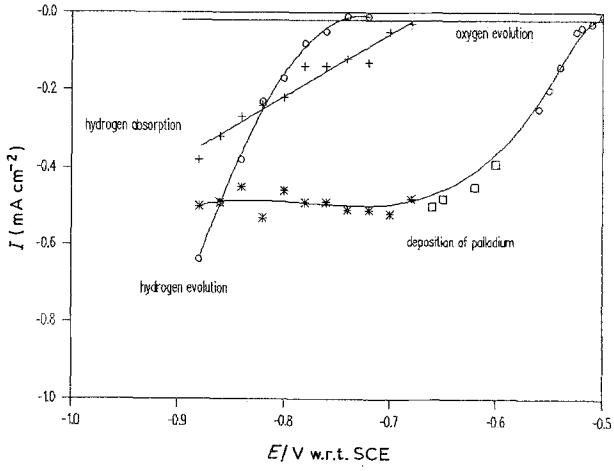

Fig. 8. Partial current densities as a function of potential for oxygen reduction, palladium hydride formation (+ + +), hydrogen evolution (OOO) and palladium deposition (O□*) in an unstirred air saturated palladium electroplating bath. The electrolyte is 10 mmol dm^{-3} [Pd(NH_3)$_2$Cl$_2$] + 1 mol dm^{-3} NH_4Cl pH 8.6. On the Pd deposition curve the different symbols indicate the slightly pulse sequences used to estimate the partial current density (see text).

assuming that the rate of the process is uniform throughout the deposition process) and also the estimate of the oxygen reduction current if the electrolyte is air sparged.

4. Discussion

Several features of palladium electroplating baths can be deduced from the above data. Whatever the pH of the electrolyte, complexing agents must be present to ensure the chemical stability of the palladium(II) species in the bath. On the other hand, the interaction of the ligands with the palladium(II) must not be too strong or the potential of the Pd(II)/Pd couple will be shifted negative into the region where palladium hydride will be formed, leading to the degradation of the mechanical and physical properties of the deposit. In the case of the bath studied here, the palladium is stabilized by the formation of $[Pd(NH_3)_4]^{2+}$ and there is no evidence of hydrolysis or other decomposition reactions. Moreover, although the potential window for palladium deposition without hydride formation is only about 150 mV, the deposition of an adherent, smooth deposit will surely require a current density well below mass transport control and hence a potential in the range -0.50 V to -0.55 V against SCE. Hence, in plating practice, hydrogen evolution and palladium hydride formation will only be a problem if the bath is out of control. In contrast, oxygen reduction will always occur at a mass transport controlled rate on the surface of the depositing palladium. Indeed, in a bath containing only 1 g dm^{-3} Pd(II), it will lower the current efficiency substantially (20 to 50%, depending on the selected current density, see Fig. 8), but if the bath contains 10 g dm^{-3} Pd(II), the loss will be proportionately lower.

The data from the experiments at the rotating disc show that strong convection can lead to a large increase in the limiting current for palladium plating (a factor up to 50). This will also increase the maximum current density for quality palladium deposition. This increase in the plating rate will, however, be at the expense of a loss in current efficiency if the convection is introduced by air sparging; at the potentials likely to be used for electroplating, oxygen reduction is fully mass transport controlled, but palladium deposition only partially so.

Clearly, at sufficiently negative potentials, the reduction of palladium(II) can be mass transport controlled. The rather steep wave for the reaction in Fig. 8, $E_{3/4} - E_{1/4} = -52$ mV, suggests that either the Pd(II)/Pd couple is rapid and the shape of the curve is determined by the Nernst equation or the rate determining step in the electron transfer process is the second electron transfer, that is

$$Pd(II) + e^- \xrightarrow{\text{fast}} Pd(I) \quad (2)$$

$$Pd(I) + e^- \xrightarrow{\text{r.d.s.}} Pd \quad (3)$$

The distinction must await further studies.

Acknowledgement

The authors thank Johnson Matthey Materials Technology Division, Royston, Hertfordshire, for financial support of this work and Mr Peter Skinner (Johnson Matthey) for advice and encouragement throughout the programme.

References

[1] R. F. Vines, R. H. Atkinson and F. H. Reid, in 'Modern Electroplating' (edited by F. A. Lowenheim), Wiley, New York (1974).
[2] Ch. J. Raub, *Platinum Metals Rev.* **26** (1982) 158.
[3] H. D. Hedrich and Ch. J. Raub, *Metalloberflache* **31** (1977) 512.
[4] S. Jayakrishnan and S. R. Natarajan, *Metal Finishing* **88** (1988) 81.
[5] H. D. Hedrich and Ch. J. Raub, *Surf. Technol.* **8** (1979) 347.
[6] J. N. Crosby, J. A. Harrison and T. A. Whitfield, *Electrochim. Acta* **27** (1982) 897.
[7] M. F. Bell and J. A. Harrison, *J. Electroanal. Chem.* **41** (1973) 15.
[8] J. A. Harrison, R. P. J. Hill and J. Thompson, *ibid.* **47** (1973) 431.
[9] J. A. Harrison, H. B. Sierra Alcazar and J. Thompson, *ibid.* **53** (1974) 145.
[10] J. N. Crosby, J. A. Harrison and T. A. Whitfield, *Electrochim. Acta* **26** (1981) 1647.
[11] A. Razaq, PhD Thesis, University of Southampton (1983).
[12] R. Greef, R. Peat, L. M. Peter, D. Pletcher and J. Robinson, 'Instrumental Methods in Electrochemistry', Ellis Horwood, Chichester (1985).
[13] A. J. Poe and D. H. Vaughan, *Inorg. Chem. Acta* **1** (1967) 255.
[14] L. Rasmussen and C. K. Jorgensen, *Acta Chem. Scand.* **22** (1968) 2313.